LANGMUIR Article
Cite This: Langmuir 2018, 34, 2716−2724
pubs.acs.org/Langmuir

Correlation of Surface Adsorption and Oxidation with a Floatability Difference of Galena and Pyrite in High-Alkaline Lime Systems

Xiaopeng Niu,[†,§] Renman Ruan,[*,†] Liuyin Xia,[‡] Li Li,[†] Heyun Sun,[†] Yan Jia,[†] and Qiaoyi Tan[†]

[†]CAS Key Laboratory of Green Process and Engineering, Institute of Process Engineering, Chinese Academy of Sciences, Beijing 100190, China

[‡]Surface Science Western, Research Park, University of Western Ontario, London, Ontario N6G0J3, Canada

[§]University of Chinese Academy of Sciences, Beijing 100049, China

ABSTRACT: When it comes to Pb−Zn ores with high amounts of pyrite, the major problem encountered is the low separation efficiency between galena and pyrite. By virtue of high dosage of lime and collector sodium diethyl dithiocarbamate (DDTC), pyrite and zinc minerals are depressed, allowing the galena to be floated. However, there have been significant conflicting reports on the flotation behavior of galena at high pH. In this context, correlation of the surface adsorption and oxidation with the floatability difference of galena and pyrite in high-alkaline lime systems would be a key issue for process optimization. Captive bubble contact angle measurements were performed on freshly polished mineral surfaces in situ exposed to lime solutions of varying pH as a function of immersion time. Furthermore, single mineral microflotation tests were conducted. Both tests indicated that the degree of hydrophobicity on the surfaces of galena and pyrite increased in the presence of DDTC at natural or mild pulp pH. While in a saturated lime solution, at pH 12.5, DDTC only worked for galena, but not for pyrite. Surface chemistry analysis by time-of-flight secondary ion mass spectrometry (Tof-SIMS) confirmed the preference of DDTC on the galena surface at pH 12.5, which contributed to a merit recovery. Further important evidence through measurements of Tof-SIMS, ion chromatography, and high-performance liquid chromatography indicated that in high-alkaline lime systems, the merit floatability of galena could exclude the insignificant contribution of elemental sulfur (S_8) and was dominantly attributed by the strong adsorption of DDTC. In contrast, the poor flotation response of pyrite at high pH was due to the prevailing adsorption of $CaOH^+$ species. This study provides an important surface chemistry evidence for a better understanding of the mechanism on the better selectivity in the galena−pyrite separation adopting high-alkaline lime systems.

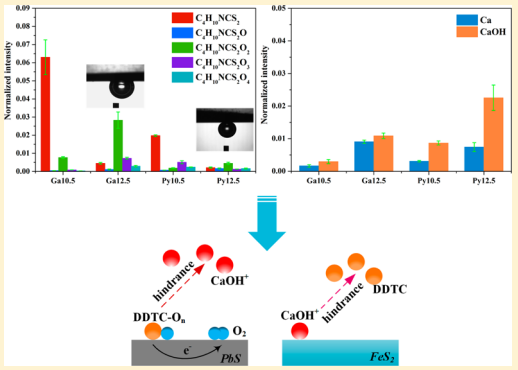

INTRODUCTION

The flotation separation of Pb−Zn sulfide ores which often occur as galena and sphalerite, associated with varying amounts of pyrite, is undoubtedly an important issue in mineral processing. Extensive investigations have focused on understanding selectively separating galena, sphalerite, and pyrite by flotation, employing flotation experiments, adsorption studies,[1−3] electrochemical techniques,[4−8] and surface analysis,[9−11] to name a few. It has been recognized that there is a link between mineral floatability, separation efficiency, and the mineral surface properties.[12−14] When it comes to Pb−Zn ores with a considerable proportion of pyrite, the major problem encountered is the low separation efficiency between galena and pyrite. The technique adopted in Fankou and Xitieshan metallurgical concentrators to warrant Pb−Zn ores with high amounts of pyrite description is the one whereby in high-alkaline lime systems (pH 12.5) with collector sodium diethyl dithiocarbamate (DDTC), pyrite and zinc minerals are depressed, allowing the galena to be floated. They were successful in practice, but little attention has been given to the study of the sulphide mineral floatability and the surface chemistry control strategy.

The main confliction happens on galena flotation behaviors as it is widely accepted that pyrite shows a very poor flotation response at high pH.[15] Disagreement concerning the flotation behavior of galena is summarized (Table 1).

Although different collectors would be expected to result in different flotation responses under the complex flotation solution environment, at high pH values above 12, there is a lack of clarity and clear link on the flotation separation of galena from pyrite and their associated surface chemistry. Notably, there have been claims that, under some circumstances, the sulfur oxidation products such as element sulfur (S_8) and polysulfide (S_n^{2-}), because of surface oxidation, could certainly render sulfide minerals floatable even without a collector.[22,25] Basically, surface oxidation was suggested to alter the chemical and physical characteristics of the sulfide mineral surface[4] and

Received: December 10, 2017
Revised: January 28, 2018
Published: January 29, 2018

DOI: 10.1021/acs.langmuir.7b04189
Langmuir 2018, 34, 2716−2724

Table 1. Summary of the Galena Flotation Behavior in Various Conditions

observed flotation response	collector	scale	references
galena only floated in the acidic condition (pH < 7)	NaEX	laboratory	Göktepe[15]
galena recovery dropped from nearly 100% at pH 5 to 60% at pH 10	DTPINa	laboratory	Pecina-Treviño et al.[16]
more than 80% of galena was recovered in the pH range 6−10	KEX	laboratory	Popov and Vučinić[17]
galena recovery was decreased slowly from 90% at pH 8 to 80% at pH 12	DDTC	laboratory	Liu et al.[18]
galena recovery exceeded 80% at pH above 12	DDTC	plant	Gu[19]
more than 80% of galena recovery was obtained from pH 4 to 12	KBX	laboratory	Gu[19]
the overall galena recovery did not exceed 50% at pH 9 for 20 min	SEDTC or SIBDTC	laboratory	Mcfadzean et al.[20]
88.9% of galena recovery was obtained at pH 9	SEDTC	laboratory	Mcfadzean et al.[21]
galena was depressed at pH values above 11 resulting from the formation of lead hydroxyl species	NaEX	plant	Ralston[22]
galena recovery increased from 50% at pH 9 to 70% at pH 10.5 and decreased to 60% at pH 12	KAX	laboratory	Ikumapayi et al.[23]
at pH 12, galena recovery was still 70% using NaOH as pH modifiers, whereas it dropped to nearly zero with CaO to adjust pH	KEX	laboratory	Liu and Zhang[24]

influence the collector interaction,[22] thus affecting surface floatability. However, at high pH values above 12, the behavior of surface oxidation of sulfide mineral remains unclear. In the presence of DDTC, Gu[19] and Sun[26] proposed that the products lead diethyl dithiocarbamate (PbD_2) and S_8 rendered galena highly floatable at pH 12.5, but their cyclic voltammetry (CV) results lacked in convincing surface chemistry evidence. Next, an important fact in practice to be considered is that the solution environment in the process of grinding is quite different from that of flotation. The milling environment was believed to be more anoxic through galvanic interactions, by which the noble sulfide minerals will be protected from oxidation because of the sacrificial dissolution of the active grinding media of iron.[27−30] Therefore, the surface oxidation of sulfide minerals is most likely inhibited in practical grinding circuits. However, in a laboratory, sample preparation involving wet grinding and ultrasonic cleaning with water could result in considerable surface oxidation prior to flotation, influencing the floatation behavior of sulfide minerals.[31−33] These conflicting reports concerning the flotation behavior of galena might have neglected this significant fact.

The contact angle is quite useful and straightforward in measuring the floatability of minerals. However, compared with the commonly reported sessile drop method,[3,11,34] the captive bubble method could mimic the process of bubble-mineral surface attachment and measure the contact angle in situ under conditions close to flotation.[35,36] For identifying and understanding the mineral surface chemistry, time-of-flight secondary ion mass spectrometry (Tof-SIMS) is quite a highly sensitive and precision technique, as it can provide elemental and molecular information from the surface species of outmost layers, that is, 1−2 atomic layers.[37−39] In this study, employing collector DDTC, the floatability of galena and pyrite was evaluated by the captive bubble contact angle method and the single mineral flotation test. ToF-SIMS analysis was utilized to investigate the interaction between the mineral surface and DDTC. The amounts of the sulfur species occurring in the course of mineral surface oxidation were determined by ion chromatography (IC) and high-performance liquid chromatography (HPLC). The primary goals of this work are, in a simulated high-alkaline lime flotation solution environment, to correlate the surface adsorption and oxidation with the floatability difference of galena and pyrite.

MATERIALS AND METHODS

Reagents. The collector DDTC [$(C_2H_5)_2NCS_2Na$, 99%] was purchased from Aladdin Industrial Corporation. Sodium sulfite (Na_2SO_3, 99%) and sodium thiosulfate ($Na_2S_2O_3$, 99%) were purchased from Sinopharm Chemical Reagent Co., Ltd. Sulfur sublimed (S^0, 99%) and calcium oxide (CaO, 98%) were purchased from Xilong Scientific Co., Ltd.

Sample Preparation. Highly pure natural specimens of galena and pyrite were obtained from the Xiling Mine (Gongcheng, Guangxi Province) and the Banlao Mine (Gengma, Yunnan Province), respectively.

In this work, first and most important, special care was given for sample preparation to ensure the minimum surface oxidation prior to the experiment. For contact angle measurements and Tof-SIMS analyses, the minerals cut into rectangular slices approximately 15 × 10 × 5 mm were embedded in an epoxy resin, grinded using 20, 10, 9 μm abrasive discs under water in sequence, and polished consecutively using 6, 3, and 1 μm diamond abrasive pads (Buehler grinder/polisher). Prior to measurements, the samples were polished on a fine polishing cloth with 0.04 μm colloidal SiO_2 and finished by polishing on the soft suede cloth using an ethanol suspension of 0.03 μm aluminum oxide. After these steps, the samples were rinsed in deoxygenated deionized water, ultrasonically cleaned with ethanol and dried under a stream of dry argon.

The minerals were ground in a nitrogen glovebox using an agate mortar and pestle and then were dry-screened to obtain +38−74 μm size fractions for microflotation tests, IC, and HPLC measurements.

In Situ Contact Angle Measurement. The contact angles of freshly polished mineral surfaces immersed in lime solutions were measured by the captive bubble method in a quartz cell utilizing a contact angle goniometer (DM-701, Kyowa Interface Science, Japan), and a schematic diagram is shown in Figure 1. By exposing the mineral surfaces to $Ca(OH)_2$ solutions of varying pH values with and without DDTC, equilibrium contact angles were monitored over the immersion time in situ (i.e., by keeping the surfaces in solution and not exposing them to air, and the values, which were recorded every 20 s for 80 s upon the contact of the air bubble and the mineral surface, were averaged and reported as the equilibrium contact angle). At least three measurements were taken and averaged.

Microflotation Tests. A custom-made Hallimond tube (Figure 2) was employed to perform the single mineral microflotation tests. One gram of the powder mineral (−74 + 38 μm) was added to 40 mL of deionized water and conditioned for 2 min, during which the desired pH was adjusted with saturated $Ca(OH)_2$ solution. Afterward, the suspension was conditioned with DDTC for 3 min and further for 1 min, followed by flotation for 4 min. Both the float and sink fractions were collected, dried, and weighed. For each result, at least three repeated tests were conducted to obtain the average recovery.

Time-of Flight Secondary Ion Mass Spectrometry. Tof-SIMS measurements were performed using an ION-TOF, TOF SIMS IV

DOI: 10.1021/acs.langmuir.7b04189
Langmuir 2018, 34, 2716−2724

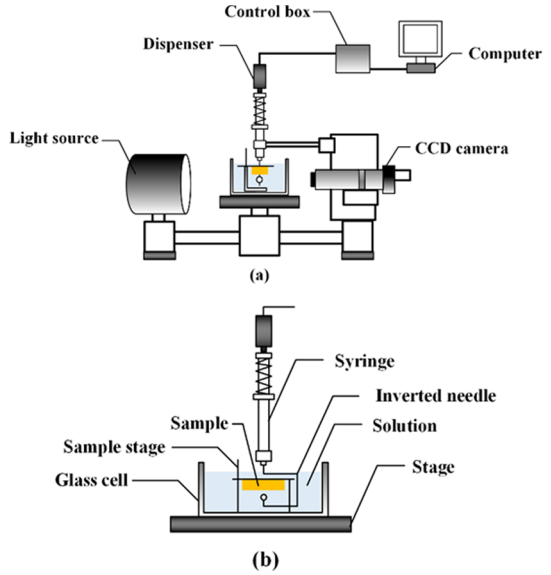

Figure 1. (a) Schematic of the experimental setup. (b) Configuration of in situ contact angle measurement.

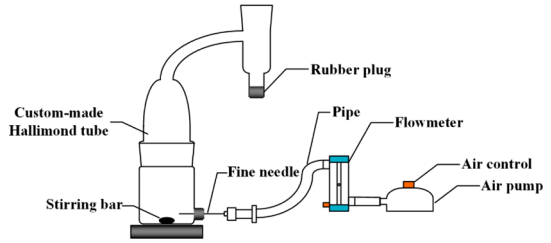

Figure 2. Experimental setup of microflotation.

secondary ion mass spectrometer to analyze the outermost layer of surface of minerals. A pulsed liquid metal Bi^{3+} primary ion beam operating at 25 kV was used to sputter and ionize species from a sample surface, and three representative regions on each sample were examined. The intensities of the surface components for regions of interest as positive and negative secondary ions were expressed by average values with the error bars. For each region of interest, data presented (counts) were normalized by the total ion intensity (counts of the recorded total mass spectrum).

The freshly polished surfaces of galena and pyrite were conditioned separately for 20 min in 50 ppm DDTC solution at the desired pH adjusted by saturated $Ca(OH)_2$ solution. Afterward, these samples were removed from the solution and blew with dry argon and immediately introduced into the fore-vacuum chamber of the Tof-SIMS instrument.

IC and HPLC. One gram of the powder mineral (−74 + 38 μm) was conditioned in the constant desired pH values of 40 mL of lime solution for 20 min. After centrifugation for 5 min at 9000 rpm, the supernatant was decanted to determine the concentrations of $S_2O_3^{2-}$, SO_3^{2-}, and SO_4^{2-} by IC (ICS-5000+ DC, Dionex). For the determination of S_8, 10 mL of ethanol was added to the pellet of the centrifugation to extract S_8 on the mineral surface, followed by 10 min of ultrasonic treatment and subsequent 5 min of centrifugation.[40] Afterward, the supernatant was quantitatively decanted to measure S_8 by HPLC (SPD-M20A, Shimadzu Corporation).

RESULTS

Assessment of Floatability. Figure 3 shows the contact angle results as a function of the immersion time in lime solutions of varying pH values with and without collector DDTC. Generally, the contact angles do not show any significant change with the increasing immersion time. This indicates the fast adsorption kinetics of DDTC. Of greater contrast is the effect of pH and collector DDTC. At pH 8.5 and 10.5, the degree of hydrophobicity on the galena and pyrite surface increased in the presence of DDTC, while in the case of high dosage of lime, at pH 12.5, DDTC exhibited a characteristic change in mineral hydrophobicity only on galena but not on pyrite. The contact angle data were further verified by single mineral flotation (Table 2). Both of these results pointed that in the presence of DDTC, the action of high dosage of lime (pH 12.5) dramatically decreased floatability of pyrite, whereas galena was slightly affected. Importantly, the enhancement of the difference in mineral floatability would result in much better separation selectivity.

Identification of Surface Adsorption and Oxidation. Figure 4 shows the normalized intensities for mass positions of five most relevant diagnostic peaks indicative of the collector DDTC adsorption on galena and pyrite surfaces. The most significant diagnostic peak for DDTC on the galena surface is $C_4H_{10}NCS_2$ at pH 10.5 and $C_4H_{10}NCS_2O_2$ at pH 12.5 (Figure 4a). This suggests that changes of solution conditions such as pH values alter the configuration of DDTC adsorption on the galena surface. A similar behavior was observed on the pyrite surface. For comparison, to provide quantitative information of DDTC adsorption on mineral surfaces, these accumulative normalized intensities of five diagnostic peaks are illustrated in Figure 4b. As noted, the galena surface showed obviously higher accumulative normalized intensities than the pyrite surface both at pH 10.5 and 12.5, indicating the stronger adsorption of DDTC on galena. Further evidence for better selectivity exhibited by DDTC in the separation of galena from pyrite at pH 12.5 than pH 10.5 is given in Table 3, which is consistent with the floatability results (Table 2).

Figure 5 shows the normalized intensities of Ca species. The control test was carried out in identical solution conditions without DDTC. For both the control test and the 50 ppm DDTC addition test, a higher intensity of the calcium signal was found at pH 12.5 than 10.5. This result is particularly evident for pyrite, indicating the stronger affinity of the hydrophilic calcium species toward the pyrite surface at high pH. Notably, the $CaOH^+$ secondary ions do not necessarily represent calcium hydroxyl species $CaOH^+$ because of the complex relationship between secondary ions and the actual species present at the surface.[41] However, in light of the calcium species distribution diagram[42] and the relevant literature,[43] the most predominant calcium species is $CaOH^+$ or Ca^{2+} at a pH range of 12−13. Thus, most $CaOH^+$ secondary ions would be expected to be from calcium hydroxyl species $CaOH^+$.

The main negative secondary ions involved in sulfur oxidation of mineral surfaces are presented in Figure 6. Truly, unequivocally identifying the source of S atoms in these parent and fragment secondary ions is difficult. Nevertheless, according to the IC and HPLC results (Table 4), the major oxidized sulfur products of surfaces of galena and pyrite in alkaline solutions are sulfoxy species (e.g., $S_2O_3^{2-}$, SO_3^{2-}, and SO_4^{2-}) rather than element sulfur (S_8), in contrast to that in acidic solutions.[44] Therefore, the intense S and HS signals observed in secondary ions (Figure 6) should not mainly derive from S_8. Besides S and SH signals (Figure 6), both the tests with and without the DDTC addition were found the SO_3 secondary ions, the indicator of sulfide mineral sulfur oxidation,[27,45] predominantly on the mineral surfaces. It should

DOI: 10.1021/acs.langmuir.7b04189
Langmuir 2018, 34, 2716−2724

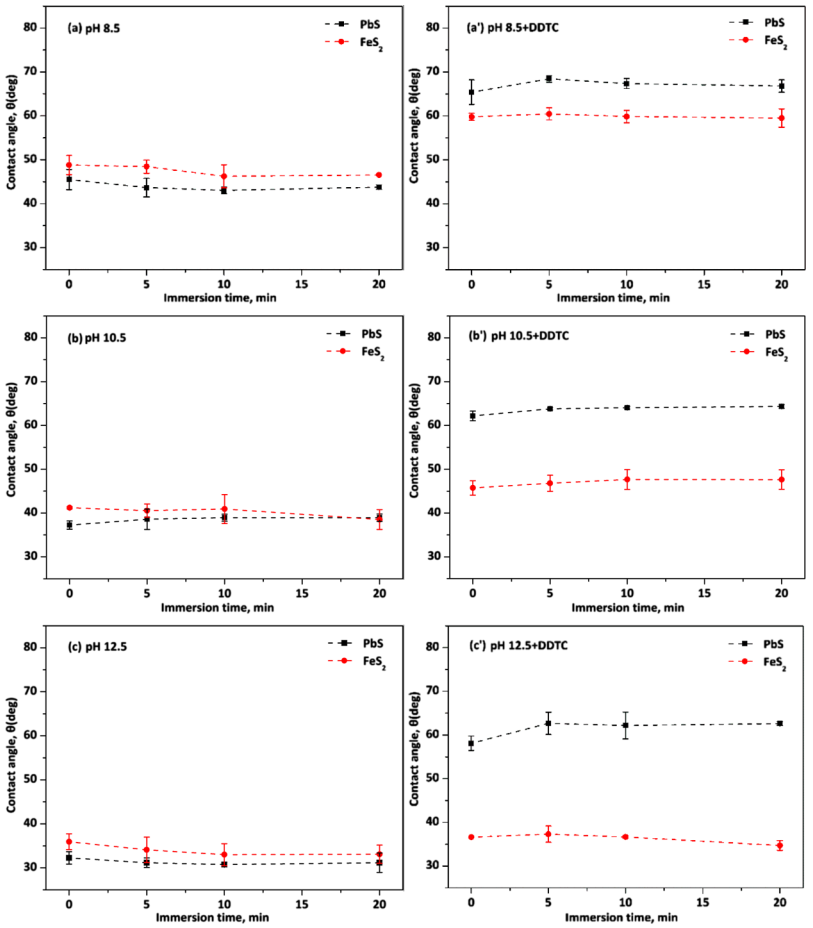

Figure 3. Contact angles of surfaces of galena and pyrite in lime solutions with varying immersion times for (a) pH 8.5, (b) pH 10.5, and (c) pH 12.5 without DDTC and for (a′) pH 8.5, (b′) pH 10.5, and (c′) pH 12.5 with 50 ppm DDTC.

Table 2. Contact Angles of Galena (Ga) and Pyrite (Py), Their Contact Angle Difference, Recovery, and Separation Selectivity[a]

		average contact angle (deg)		contact angle difference (deg)	recovery (%)		separation selectivity
conditions	Eh (mV vs SHE)	Ga	Py	$\theta_{Ga} - \theta_{Py}$	Ga	Py	R_{Ga}/R_{Py}
pH 8.5	478	44.0	47.5	−3.5	38.5	28.0	1.4
pH 8.5 + DDTC	318	67.0	59.9	7.1	95.0	69.0	1.4
pH 10.5	446	38.4	40.3	−1.9	34.0	23.0	1.5
pH 10.5 + DDTC	311	63.6	47.0	16.6	91.0	58.5	1.6
pH 12.5	202	31.4	34.0	−2.6	9.5	---	---
pH 12.5 + DDTC	196	61.4	36.3	25.1	86.0	---	---

[a]--- indicates not detected.

be emphasized that the SO_3 secondary ions could arise from sulfoxy species and not necessarily be sulfite. Further, in the control tests (no DDTC addition) (Figure 6a′,b′), notable sulfoxy secondary ions were still observed, confirming the formation of sulfoxy species during the sulfur oxidation of sulfide mineral surfaces in alkaline solutions. Overall, there does not exist a significant difference in the sulfur oxidation behavior between galena and pyrite at pH 12.5, as evidenced by their similar distribution trend in Tof-SIMS analysis (e.g., the marked SO_3 secondary ions) along with the total sulfur oxidation data of IC/HPLC results. This might indicate the similar sulfur oxidation mechanism/rate of galena and pyrite in high-alkaline conditions.

DISCUSSION

The surface oxidation of sulfide mineral is an electrochemical process, and its impact on the flotation performance remains debatable.[25,46] Such an electrochemical process involves three steps including cathodic reaction, electron transport, and anodic reaction. As pointed out by Rimstidt and Vaughan,[47] the key to understanding sulfide mineral oxidation is complicated by the oxidation of the sulfur atom occurring as anodic reaction. Indeed, a primary problem is the fact that the anodic reaction of seven electrons from disulfide or eight electrons from sulfide sulfur forming sulfate might involve different intermediate sulfur oxidation products.[27] Ralston mentioned that galena ground under the suitable conditions could float in the absence of collector because of the hydrophobic role of sulfur oxidation products such as element

DOI: 10.1021/acs.langmuir.7b04189
Langmuir 2018, 34, 2716−2724

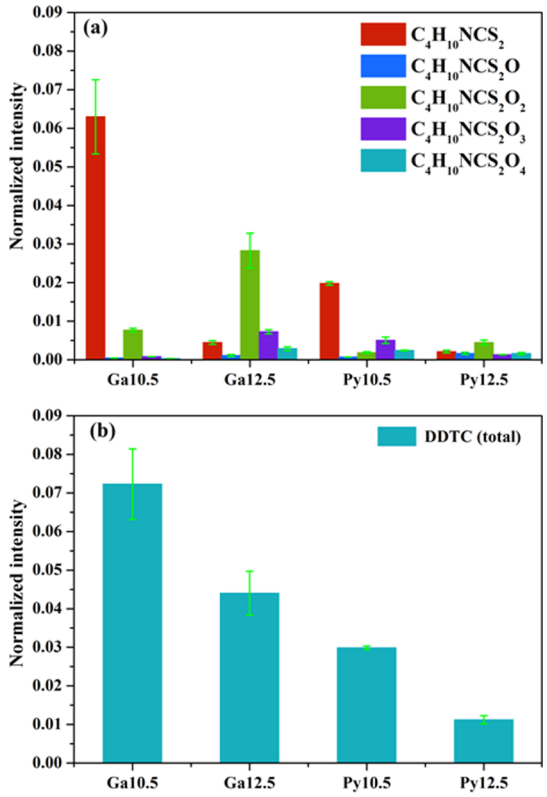

Figure 4. Tof-SIMS-normalized intensities of DDTC adsorption on surfaces of galena (Ga) and pyrite (Py) with the 50 ppm DDTC addition at pH 10.5 and 12.5: (a) spectral fingerprints for DDTC (negative secondary ions) and (b) accumulative normalized intensities of DDTC.

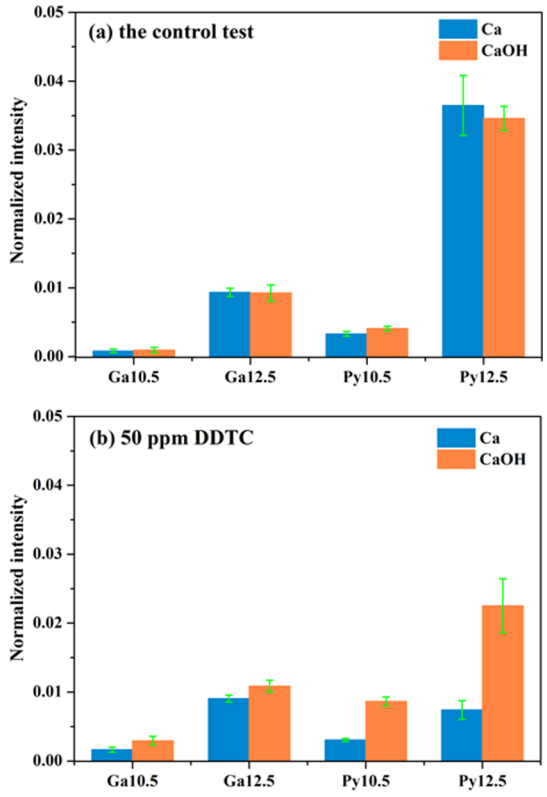

Figure 5. Tof-SIMS-normalized intensities of Ca species (positive secondary ions) on galena (Ga) and pyrite (Py) surfaces at pH 10.5 and 12.5 from the (a) control test (no DDTC addition); (b) test with the 50 ppm DDTC addition.

Table 3. Accumulative Normalized Intensities of DDTC on Galena (I_{Ga}) and Pyrite (I_{Py}) and Their Ratios

conditions	I_{Ga}	I_{Py}	I_{Ga}/I_{Py}
pH 10.5 + 50 ppm DDTC	0.07228	0.02986	2.4
pH 12.5 + 50 ppm DDTC	0.04405	0.01123	3.9

sulfur (S_8) and polysulfide (S_n^{2-}).[22] According to CV results, Gu proposed that both lead diethyl dithiocarbamate (PbD_2) and S_8 contributed to the strong floatability of galena in high-alkaline lime systems (pH 12.5) but provided no evidence to identify these products.[19] However, the hydrophobic role of S_8 at such high pH values is in doubt because of its thermodynamics and kinetics unstability in an alkaline medium.[48] Importantly, at pH 12.5, the main sulfur species of galena surfaces oxidation were sulfoxy species rather than S_8 (Table 4 and Figure 6). Together, at pH 12.5, the insignificant hydrophobic role of galena surface oxidation products was further evidenced by the slight contact angle changes with the immersion time in the absence of DDTC (Figure 3), as well as its poor recovery without DDTC (Table 2).

It is well-known that $S_2O_3^{2-}$ is thought to be the first liberated sulfur compound during aqueous pyrite oxidation by O_2 at a pH range of 2−9.[49−51] Only the significantly accelerated decomposition rates of $S_2O_3^{2-}$ were observed on the addition of pyrite, as well as the similar observation in the presence of galena and sphalerite, and a surface-catalyzed $S_2O_3^{2-}$ oxidation mechanism was postulated.[52] Inspired by previous studies, on the basis of our Tof-SIMS and IC/HPLC results (Figure 6 and Table 4), a surface reaction model is proposed in Figure 7 to explain the evolution of sulfur species in the course of mineral surface oxidation in alkaline solutions.

As noted in Figure 7, the evolution process of sulfur species includes cathodic reaction (i.e., the reduction of O_2), electron transport, and anodic reaction (i.e., the oxidation of sulfur). Although the details of the electron transfers and intermediate sulfur species are not clear, the reactions leading to the sulfur species may be represented as follows:[53,54]

$$S_2O_3^{2-} + 2OH^- + O_2 \rightarrow 2SO_3^{2-} + H_2O \quad (1)$$

$$2SO_3^{2-} + O_2 \rightarrow 2SO_4^{2-} \quad (2)$$

The transport of electrons is expected to play a key role in determining the surface sulfur oxidation rate. Further, the sulfur species actually present at the surface are in fact the resultant of surface oxidation, adsorption, and desorption.

Of most interest is the interpretation of the different DDTC adsorption behaviors on galena and pyrite under similar solution environments. An important fact to be considered is the much more $CaOH^+$ secondary ions on the pyrite surface than on the galena surface at pH 12.5 (Figure 5), indicating a stronger affinity of the hydrophilic calcium species toward pyrite. In the case of $CaOH^+$ adsorption on the pyrite (100) surface, through density functional theory (DFT) calculations, both the O atom of the −OH group and the Ca atom could occupy the active Fe sites which were claimed for thiol collectors adsorption.[55,56] Inspired by these literature, at high pH, the active Fe sites for DDTC adsorption would be expected to notably decrease because of the prevailing adsorption of considerable calcium species in the course of

DOI: 10.1021/acs.langmuir.7b04189
Langmuir 2018, 34, 2716−2724

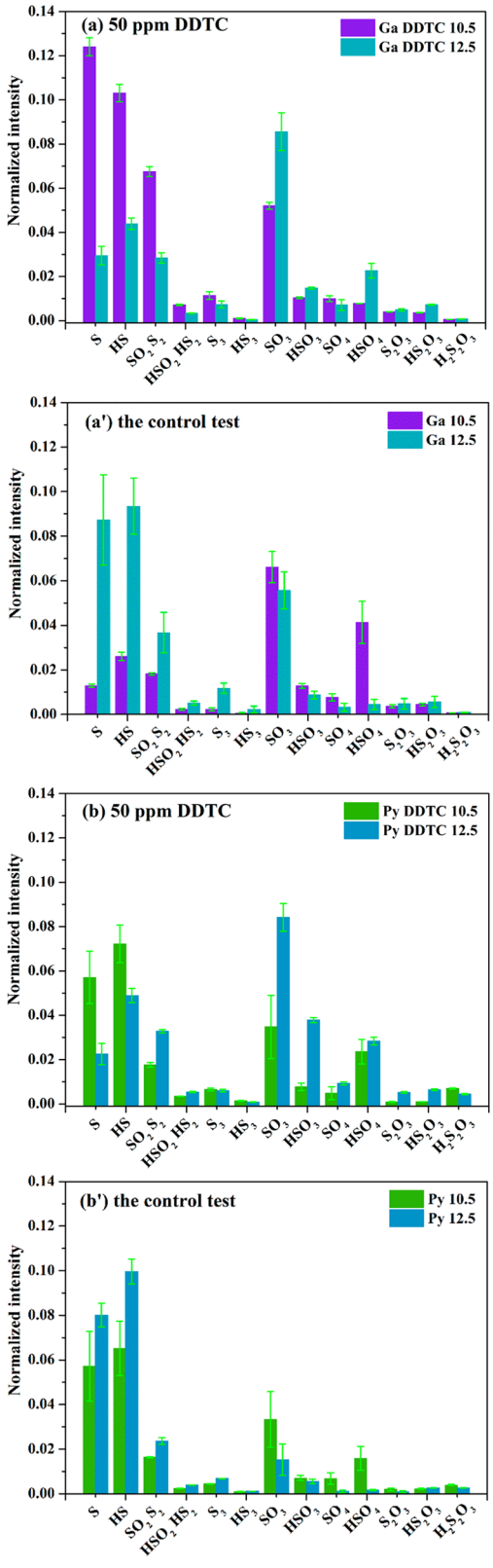

Figure 6. Tof-SIMS-normalized intensities of sulfur species (negative secondary ions) from galena (Ga) (a) with 50 ppm DDTC addition, (a′) the control test (no DDTC addition) and pyrite (Py), (b) with 50 ppm DDTC addition, and (b′) the control test (no DDTC addition) at pH 10.5 and 12.5, respectively.

competitive adsorption between calcium hydroxyl species (e.g., $CaOH^+$) and DDTC. Additionally, the key role of $CaOH^+$ species adsorption on pyrite depression was further evidenced by the similar surface oxidation behavior but obviously different flotation responses of pyrite at pH 10.5 and 12.5 (Table 4 and Figure 6). Therefore, the significant depression of pyrite at pH 12.5 is explained with the prevailing adsorption of $CaOH^+$ species in the competitive adsorption between $CaOH^+$ species and DDTC, resulting in a diminished interaction between DDTC and the pyrite surface.

Table 4. Amounts of Sulfoxy Species in Solution and Element Sulfur on the Surfaces of Galena (Ga) and Pyrite (Py) after 20 min Conditioning at pH 10.5 and 12.5 without DDTC as Determined by IC and HPLC (mg)[a]

	Ga10.5	Ga12.5	Py10.5	Py12.5
$S_2O_3^{2-}$	0.0496	0.1292	0.1164	0.0532
SO_4^{2-}	0.0156	0.0396	0.0696	0.1052
SO_3^{2-}	---	---	0.0432	0.0572
S_8	0.0124	0.0096	0.0044	0.0008
total	0.0776	0.1784	0.2336	0.2164

[a]--- indicates not detected.

The proposed interaction mechanisms between thiol collectors and sulfide mineral surfaces are summarized as follows:

(1) Ion exchange of mineral surface oxidation products by the collector ion.[57]
(2) The reaction of dissolved metal ions from soluble surface oxidation products with the collector and subsequent precipitation of the metal thiolate complex onto the surface.[46]
(3) The formation of dithiolate at the surface if the rest potential of the metal sulfide is more than the reduction potential for the dithiolate/thiol couple under the particular conditions.[58]

At pH 12.5, pyrite and galena showed a similar surface oxidation behavior (Figure 6 and Table 4) but notably different DDTC adsorption actions. With respect to xanthate adsorption as mechanism (1), it is postulated that the oxidation of the galena surface is a prerequisite.[57] On the contrary, others refute this prerequisite and propose that oxygen and xanthate can react simultaneously with the galena surface.[59] However, our work demonstrated that the fresh galena surface still interacted strongly with DDTC (Figure 2). In contrast with the xanthate-galena system as mechanism (2), microcalorimetric investigations indicated that DDTC reacted directly with the galena surface at pH 9.[46] They explained that compared with the O atom in xanthate, the N atom in the DDTC was more positively inductive and pushed electron density toward the reactive thiol head group, therefore resulting in a stronger bond between DDTC and the mineral surface. Through DFT calculations, the interaction between xanthate S 3p and pyrite Fe 3d was stronger than that with galena Pb 6sp, whereas the interaction between DDTC S 3p and pyrite Fe 3d was weaker than that with galena Pb 6sp.[56] Further, the absence of the diagnostic peak for tetraethyl thiuram disulfide $(DTC)_2$ (Figure 4) does not favor the mechanism (3). Therefore, at natural or mild pulp pH, the interaction mechanism is explained with the adsorption of DDTC ions (X^-) directly onto the galena surface.

At pH 12.5, the most intense diagnostic peak of DDTC adsorption on galena varied from $C_4H_{10}NCS_2$ to $C_4H_{10}NCS_2O_2$, indicating the changes of DDTC adsorption configuration on the surface. Changes of solution conditions

DOI: 10.1021/acs.langmuir.7b04189
Langmuir 2018, 34, 2716−2724

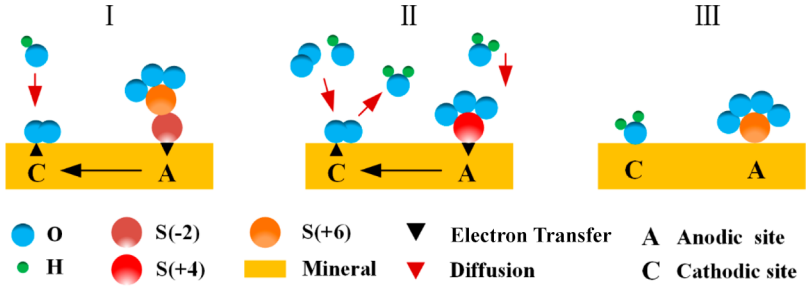

Figure 7. Schematic of the evolution process of surface sulfur oxidation. (I) Electrons are transferred from $S_2O_3^{2-}$ produced on the anodic sites (A) via the conduction bands of mineral to O_2 sorbs on the cathodic sites (C); (II) electrons are transferred from SO_3^{2-} as a result of $S_2O_3^{2-}$ oxidation via the conduction bands of mineral to O_2; (III) formation of SO_4^{2-} due to SO_3^{2-} oxidation.

(e.g., pH or Eh) exert a profound effect on collector adsorption and modify the interaction between the mineral surface and the thiol collector, thus altering the configuration of DDTC adsorption on the mineral surface. The source of the O atom in $C_4H_{10}NCS_2O_2$ was expected to originate from the dissolved oxygen during the adsorption of DDTC ions (X^-) on the galena surface which behaved as a catalyst to transfer electrons:

$$X^- + nO_2 \rightarrow (X - O_n)_{ads}^- \quad (3)$$

The good floatability of galena at high pH could be contributed to the prevailing adsorption of DDTC in the course of competitive adsorption between $CaOH^+$ species and DDTC. Our preliminary results of DFT calculations also indicated that the adsorption energy of $CaOH^+$ on the pyrite (100) surface (i.e., −281.13 kJ/mol) was larger than that on the galena (100) surface (i.e., −204.23 kJ/mol), supporting a higher affinity of $CaOH^+$ on pyrite. Further, the different performance of $CaOH^+$ and DDTC in the course of competitive adsorption on galena and pyrite surfaces was considered to be arising from the differences in their surface configuration and electronic structure.[60,61]

CONCLUSIONS

The motivation of this study is the unclear depressive mechanism of lime in the flotation separation of galena from pyrite at high pH values using collector DDTC. Indeed, the floatation response was different for galena and pyrite in high-alkaline systems relative to mild conditions which could be orientated by their surface adsorption and oxidation. Both the in situ contact angle results and single mineral flotation data showed that the effect of collector DDTC was much related to pulp pH. The action of high dosage of lime (pH 12.5) dramatically decreased floatability of pyrite, whereas the recovery of galena was only slightly affected. Tof-SIMS investigation confirmed that although pH variations altered the configuration of DDTC on the mineral surface, the adsorption of DDTC on galena was stronger than that on pyrite both at pH 10.5 and 12.5. Studies through Tof-SIMS analysis, IC, and HPLC measurements indicated that in high-alkaline lime systems, the merit floatability of galena could exclude the insignificant contribution of elemental sulfur and was dominantly attributed to the strong adsorption of DDTC. The depression of pyrite at high pH was explained with the prevailing adsorption of $CaOH^+$ species during the competitive adsorption between $CaOH^+$ species and DDTC anions. This study provides an important surface chemistry evidence for the good floatability of galena and the significant pyrite depression at high pH and for understanding the mechanism on the better selectivity in the galena−pyrite flotation separation adopting high-alkaline lime systems.

AUTHOR INFORMATION

Corresponding Author

*E-mail: rmruan@ipe.ac.cn. Phone: +86-10-82544972.

ORCID

Xiaopeng Niu: 0000-0003-3149-0674

Notes

The authors declare no competing financial interest.

ACKNOWLEDGMENTS

The authors are thankful for the financial support of this study by the National Natural Science Foundation of China (nos. 51674231 and 41401541), Bureau of International Co-operation, Chinese Academy of Sciences (no. 122111KYSB20150013), and Science and Technology Service Network Initiative, Chinese Academy of Sciences (no. KFJ-SW-STS-148). The assistance from Dr. Peng Xi is much appreciated for improving the microflotation setup. The constructive suggestions and comments of the manuscript reviewers are also gratefully acknowledged.

REFERENCES

(1) Vučinić, D. R.; Lazić, P. M.; Rosić, A. A. Ethyl Xanthate Adsorption and Adsorption Kinetics on Lead-Modified Galena and Sphalerite under Flotation Conditions. *Colloids Surf., A* **2006**, *279*, 96−104.

(2) Fredriksson, A.; Holmgren, A.; Forsling, W. Kinetics of Collector Adsorption on Mineral Surfaces. *Miner. Eng.* **2006**, *19*, 784−789.

(3) Wang, J.; Xie, L.; Liu, Q.; Zeng, H. Effects of Salinity on Xanthate Adsorption on Sphalerite and Bubble−Sphalerite Interactions. *Miner. Eng.* **2015**, *77*, 34−41.

(4) Hampton, M. A.; Plackowski, C.; Nguyen, A. V. Physical and Chemical Analysis of Elemental Sulfur Formation during Galena Surface Oxidation. *Langmuir* **2011**, *27*, 4190−4201.

(5) Mu, Y.; Peng, Y.; Lauten, R. A. Electrochemistry Aspects of Pyrite in the Presence of Potassium Amyl Xanthate and a Lignosulfonate-Based Biopolymer Depressant. *Electrochim. Acta* **2015**, *174*, 133−142.

(6) Qin, W.; Wang, X.; Ma, L.; Jiao, F.; Liu, R.; Yang, C.; Gao, K. Electrochemical Characteristics and Collectorless Flotation Behavior of Galena: With and Without the Presence of Pyrite. *Miner. Eng.* **2015**, *74*, 99−104.

(7) Mycroft, J. R.; Bancroft, G. M.; McIntyre, N. S.; Lorimer, J. W.; Hill, I. R. Detection of Sulphur and Polysulphides on Electrochemically Oxidized Pyrite Surfaces by X-ray Photoelectron Spectroscopy and Raman Spectroscopy. *J. Electroanal. Chem. Interfacial Electrochem.* **1990**, *292*, 139−152.

(8) Wang, J.; Liu, Q.; Zeng, H. Understanding Copper Activation and Xanthate Adsorption on Sphalerite by Time-of-Flight Secondary Ion

DOI: 10.1021/acs.langmuir.7b04189
Langmuir 2018, 34, 2716−2724

Mass Spectrometry, X-ray Photoelectron Spectroscopy, and In Situ Scanning Electrochemical Microscopy. *J. Phys. Chem. C* **2013**, *117*, 20089−20097.
(9) Mikhlin, Y. L.; Karacharov, A. A.; Likhatski, M. N. Effect of Adsorption of Butyl Xanthate on Galena, PbS, and HOPG Surfaces as Studied by Atomic Force Microscopy and Spectroscopy and XPS. *Int. J. Miner. Process.* **2015**, *144*, 81−89.
(10) Mikhlin, Y.; Karacharov, A.; Tomashevich, Y.; Shchukarev, A. Interaction of Sphalerite with Potassium n-Butyl Xanthate and Copper Sulfate Solutions Studied by XPS of Fast-Frozen Samples and Zeta-Potential Measurement. *Vacuum* **2016**, *125*, 98−105.
(11) Deng, M.; Karpuzov, D.; Liu, Q.; Xu, Z. Cryo-XPS Study of Xanthate Adsorption on Pyrite. *Surf. Interface Anal.* **2013**, *45*, 805−810.
(12) Kor, M.; Korczyk, P. M.; Addai-Mensah, J.; Krasowska, M.; Beattie, D. A. Carboxymethylcellulose Adsorption on Molybdenite: the Effect of Electrolyte Composition on Adsorption, Bubble−surface Collisions, and Flotation. *Langmuir* **2014**, *30*, 11975−11984.
(13) Xie, L.; Shi, C.; Wang, J.; Huang, J.; Lu, Q.; Liu, Q.; Zeng, H. Probing the Interaction between Air Bubble and Sphalerite Mineral Surface using Atomic Force Microscope. *Langmuir* **2015**, *31*, 2438−2446.
(14) Xie, L.; Wang, J.; Yuan, D.; Shi, C.; Cui, X.; Zhang, H.; Liu, Q.; Liu, Q.; Zeng, H. Interaction Mechanisms between Air Bubble and Molybdenite Surface: Impact of Solution Salinity and Polymer Adsorption. *Langmuir* **2017**, *33*, 2353−2361.
(15) Göktepe, F. Effect of pH on Pulp Potential and Sulphide Mineral Flotation. *Turk. J. Eng. Environ. Sci.* **2002**, *26*, 309−318.
(16) Pecina-Treviño, E. T.; Uribe-Salas, A.; Nava-Alonso, F. Effect of Dissolved Oxygen and Galvanic Contact on the Floatability of Galena and Pyrite with Aerophine 3418A. *Miner. Eng.* **2003**, *16*, 359−367.
(17) Popov, S. R.; Vučinić, D. R. The Effect of Copper Ions on Galena Floatability and Ethyl Xanthate Adsorption. *Colloids Surf.* **1990**, *44*, 191−205.
(18) Liu, R.; Guo, Y.; Wang, L.; Sun, W.; Tao, H.; Hu, Y. Effect of Calcium Hypochlorite on the Flotation Separation of Galena and Jamesonite in High-Alkali Systems. *Miner. Eng.* **2015**, *84*, 8−14.
(19) Gu, G. Oxidation-Reduction Reactions of Sulfide Minerals Grinding-Flotaion Systems and Origin Potential Flotation(OPF). Ph.D. Thesis, Central South University of Technology, Changsha, 1998.
(20) Mcfadzean, B.; Castelyn, D. G.; O'Connor, C. T. The Effect of Mixed Thiol Collectors on the Flotation of Galena. *Miner. Eng.* **2012**, *36*−*38*, 211−218.
(21) Mcfadzean, B.; Mhlanga, S. S.; O'Connor, C. T. The Effect of Thiol Collector Mixtures on the Flotation of Pyrite and Galena. *Miner. Eng.* **2013**, *50*−*51*, 121−129.
(22) Ralston, J. The Chemistry of Galena Flotation: Principles & Practice. *Miner. Eng.* **1994**, *7*, 715−735.
(23) Ikumapayi, F.; Makitalo, M.; Johansson, B.; Rao, K. H. Recycling of Process Water in Sulphide Flotation: Effect of Calcium and Sulphate Ions on Flotation of Galena. *Miner. Eng.* **2012**, *39*, 77−88.
(24) Liu, Q.; Zhang, Y. Effect of Calcium Ions and Citric Acid On the Flotation Separation of Chalcopyrite from Galena using Dextrin. *Miner. Eng.* **2000**, *13*, 1405−1416.
(25) Hu, Y.; Sun, W.; Wang, D. *Electrochemistry of Flotation of Sulphide Minerals*; Tsinghua University Press; Springer: Beijing, 2009; pp 48−52.
(26) Sun, W.; Sun, C.; Liu, R.-q.; Cao, X.-f.; Tao, H.-b. Electrochemical Behavior of Galena and Jamesonite Flotation in High Alkaline Pulp. *Trans. Nonferrous Met. Soc. China* **2016**, *26*, 551−556.
(27) Owusu, C.; e Abreu, S. B.; Skinner, W.; Addai-Mensah, J.; Zanin, M. The Influence of Pyrite Content on the Flotation of Chalcopyrite/Pyrite Mixtures. *Miner. Eng.* **2014**, *55*, 87−95.
(28) Huang, G.; Grano, S. Galvanic Interaction between Grinding Media and Arsenopyrite and its Effect on Flotation: Part I. Quantifying Galvanic Interaction during Grinding. *Int. J. Miner. Process.* **2006**, *78*, 182−197.
(29) Wei, Y.; Sandenbergh, R. F. Effects of Grinding Environment on the Flotation of Rosh Pinah Complex Pb/Zn Ore. *Miner. Eng.* **2007**, *20*, 264−272.
(30) Bruckard, W. J.; Sparrow, G. J.; Woodcock, J. T. A Review of the Effects of the Grinding Environment on the Flotation of Copper Sulphides. *Int. J. Miner. Process.* **2011**, *100*, 1−13.
(31) Jones, C. F.; LeCount, S.; Smart, R. S. C.; White, T. J. Compositional and Structural Alteration of Pyrrhotite Surfaces in Solution: XPS and XRD Studies. *Appl. Surf. Sci.* **1992**, *55*, 65−85.
(32) Nowak, P.; Laajalehto, K. Oxidation of Galena Surface—an XPS Study of the Formation of Sulfoxy Species. *Appl. Surf. Sci.* **2000**, *157*, 101−111.
(33) Kocabag, D.; Kelsall, G. H.; Shergold, H. L. Natural Oleophilicity/Hydrophobicity of Sulphide Minerals, I. Galena. *Int. J. Miner. Process.* **1990**, *29*, 195−210.
(34) Raichur, A. M.; Wang, X. H.; Parekh, B. K. Quantifying Pyrite Surface Oxidation Kinetics by Contact Angle Measurements. *Colloids Surf., A* **2000**, *167*, 245−251.
(35) Sedeva, I. Probing the Adsorption of Polymer Depressants on Hydrophobic Surfaces using the Quartz Crystal Microbalance. Ph.D. Thesis, University of South Australia, September 2009.
(36) Wang, J.; Yoon, R.-H.; Morris, J. AFM Surface Force Measurements Conducted between Gold Surfaces Treated in Xanthate Solutions. *Int. J. Miner. Process.* **2013**, *122*, 13−21.
(37) Chelgani, S. C.; Hart, B. TOF-SIMS Studies of Surface Chemistry of Minerals Subjected to Flotation Separation—A Review. *Miner. Eng.* **2014**, *57*, 1−11.
(38) Goh, S. W.; Buckley, A. N.; Gong, B.; Woods, R.; Lamb, R. N.; Fan, L.-J.; Yang, Y.-W. Thiolate Layers on Metal Sulfides Characterised by XPS, ToF-SIMS and NEXAFS Spectroscopy. *Miner. Eng.* **2008**, *21*, 1026−1037.
(39) e Abreu, S. B. Correlation of ToF-SIMS Surface Analysis with Particle Hydrophobicity and Flotation. Ph.D. Thesis, University of South Australia, November 2012.
(40) Schippers, A.; Jozsa, P.; Sand, W. Sulfur Chemistry in Bacterial Leaching of Pyrite. *Appl. Environ. Microbiol.* **1996**, *62*, 3424−3431.
(41) Goh, S. W.; Buckley, A. N.; Lamb, R. N.; Woods, R. The Ability of Static Secondary Ion Mass Spectrometry to discriminate Submonolayer from Multilayer Adsorption of Thiol Collectors. *Miner. Eng.* **2006**, *19*, 571−581.
(42) Vergouw, J. M.; Difeo, A.; Xu, Z.; Finch, J. A. An Agglomeration Study of Sulphide Minerals using Zeta-potential and Settling Rate. Part 1: Pyrite and galena. *Miner. Eng.* **1998**, *11*, 159−169.
(43) Li, Y.; Chen, J.; Kang, D.; Guo, J. Depression of pyrite in Alkaline Medium and its Subsequent Activation by Copper. *Miner. Eng.* **2012**, *26*, 64−69.
(44) Schippers, A.; Sand, W. Bacterial Leaching of Metal Sulfides Proceeds by two Indirect Mechanisms via Thiosulfate or via Polysulfides and Sulfur. *Appl. Environ. Microbiol.* **1999**, *65*, 319−321.
(45) Smart, R. S. C.; Jasieniak, M.; Prince, K. E.; Skinner, W. M. SIMS Studies of Oxidation Mechanisms and Polysulfide Formation in Reacted Sulfide Surfaces. *Miner. Eng.* **2000**, *13*, 857−870.
(46) McFadzean, B.; Moller, K. P.; O'Connor, C. T. A Thermochemical Study of Thiol Collector Surface Reactions on Galena and Chalcopyrite. *Miner. Eng.* **2015**, *78*, 83−88.
(47) Rimstidt, J. D.; Vaughan, D. J. Pyrite Oxidation: A State-of-the-Art Assessment of the Reaction Mechanism. *Geochim. Cosmochim. Acta* **2003**, *67*, 873−880.
(48) Ralston, J.; Alabaster, P.; Healy, T. W. Activation of Zinc Sulphide with Cu^{II}, Cd^{II} and Pb^{II}: III. The Mass-Spectrometric Determination of Elemental Sulphur. *Int. J. Miner. Process.* **1981**, *7*, 279−310.
(49) Moses, C. O.; Nordstrom, D. K.; Herman, J. S.; Mills, A. L. Aqueous Pyrite Oxidation by Dissolved Oxygen and by Ferric Iron. *Geochim. Cosmochim. Acta* **1987**, *51*, 1561−1571.
(50) Moses, C. O.; Herman, J. S. Pyrite Oxidation at Circumneutral pH. *Geochim. Cosmochim. Acta* **1991**, *55*, 471−482.

DOI: 10.1021/acs.langmuir.7b04189
Langmuir 2018, 34, 2716−2724

(51) Luther, G. W. Pyrite Oxidation and Reduction: Molecular Orbital Theory Considerations. *Geochim. Cosmochim. Acta* **1987**, *51*, 3193−3199.
(52) Xu, Y.; Schoonen, M. A. A. The Stability of Thiosulfate in the Presence of Pyrite in Low-Temperature Aqueous Solutions. *Geochim. Cosmochim. Acta* **1995**, *59*, 4605−4622.
(53) Chen, K. Y.; Morris, J. C. Kinetics of Oxidation of Aqueous Sulfide by Oxygen. *Environ. Sci. Technol.* **1972**, *6*, 529−537.
(54) Goldhaber, M. B. Experimental Study of Metastable Sulfur Oxyanion Formation during Pyrite Oxidation at pH 6-9 and 30 °C. *Am. J. Sci.* **1983**, *283*, 193−217.
(55) Zhao, C.; Chen, J.; Li, Y.; Huang, D. W.; Li, W. DFT Study of Interactions between Calcium Hydroxyl Ions and Pyrite, Marcasite, Pyrrhotite Surfaces. *Appl. Surf. Sci.* **2015**, *355*, 577−581.
(56) Chen, J.; Lan, L.; Chen, Y. Computational Simulation of Adsorption and Thermodynamic Study of Xanthate, Dithiophosphate and Dithiocarbamate on Galena and Pyrite Surfaces. *Miner. Eng.* **2013**, *46*, 136−143.
(57) Page, P. W.; Hazell, L. B. X-ray Photoelectron Spectroscopy (XPS) Studies of Potassium Amyl Xanthate (KAX) Adsorption on Precipitated PbS Related to Galena Flotation. *Int. J. Miner. Process.* **1989**, *25*, 87−100.
(58) Finkelstein, N. P.; Poling, G. W. The Role of Dithiolates in the Flotation of Sulphide Minerals. *Miner. Sci. Eng.* **1977**, *9*, 177−197.
(59) Prestidge, C. A.; Ralston, J.; Smart, R. S. C. The Role of Cyanide in the Interaction of Ethyl Xanthate with Galena. *Colloids Surf., A* **1993**, *81*, 103−119.
(60) Chen, J.; Chen, Y.; Long, X.; Li, Y. DFT Study of Coadsorption of Water and Oxygen on Galena (PbS) Surface: An Insight into the Oxidation Mechanism of Galena. *Appl. Surf. Sci.* **2017**, *420*, 714−719.
(61) Li, Y.; Chen, J.; Chen, Y.; Zhao, C.; Zhang, Y.; Ke, B. Interactions of Oxygen and Water Molecules with Pyrite Surface: A New Insight. *Langmuir* **2018**, *34*, 1941−1952.

DOI: 10.1021/acs.langmuir.7b04189
Langmuir 2018, 34, 2716−2724